

# SEISMIC PERFORMANCE OF HOLLOW FIBRE-REINFORCED POLYMER (FRP) PILES IN COHESIONLESS SOILS

M.A. Hosseini, M.T. Rayhani

*Geoen지니어ing Research Group, Department of Civil and Environmental Engineering – Carleton University, Ottawa, ON, Canada*



## ABSTRACT

This study focuses on investigating seismic performance of hollow Glass Fibre-Reinforced Polymer piles compared to traditional piles in dry sand deposits using shaking table tests. A series of soil-foundation models were prepared following scaling relationships that recognize the dynamic and nonlinear nature of soil-pile systems in a laminar shear box with a dimension of 1.0 m × 1.0 m and a depth of 1.0 m. Four Glass Fibre-Reinforced Polymer (GFRP) piles were manufactured and embedded as end-bearing piles within the soil and tested under different seismic input motions. The model soil was prepared by following pluviation technique inside the laminar shear container while a thin flexible latex membrane was stretched inside the container to hold the soil. Eight accelerometers along with three LVDTs, and bending strain gauges were employed to monitor the soil and piles response during each shaking test. The shaking table tests results indicate that the traditional group piles experienced larger accelerations whereas GFRP piles showed lower acceleration values and, hence, larger flexibility to deflect.

## RÉSUMÉ

Cette étude se concentre sur l'étude de la performance sismique des pieux creux en polymère renforcé de fibres de verre par rapport aux pieux traditionnels dans les dépôts de sable sec à l'aide de tests sur table à secousses. Une série de modèles de fondation de sol ont été préparés suivant des relations d'échelle qui reconnaissent la nature dynamique et non linéaire des systèmes sol-pieu dans une boîte de cisaillement laminaire d'une dimension de 1,0 m × 1,0 m et d'une profondeur de 1,0 m. Quatre pieux en polymères renforcés de fibres de verre (GFRP) ont été fabriqués et incorporés en tant que pieux porteurs dans le sol et testés sous différents mouvements d'entrée sismiques. Le sol modèle a été préparé en suivant la technique de pluviation à l'intérieur du conteneur à cisaillement laminaire, tandis qu'une fine membrane de latex souple était étirée à l'intérieur du conteneur pour contenir le sol. Huit accéléromètres ainsi que trois LVDT et des jauges de contrainte de flexion ont été utilisés pour surveiller la réponse du sol et des pieux lors de chaque test d'agitation. Les résultats des tests de la table à secousses indiquent que les pieux traditionnels du groupe ont connu des accélérations plus importantes alors que les pieux en PRFV ont présenté des valeurs d'accélération plus faibles et, par conséquent, une plus grande flexibilité pour se dévier.

## 1 INTRODUCTION

Pile foundations are widely used to support high load structures in compressible and weak ground strata throughout the world. Piles are traditionally made of concrete, steel and timber; however, there is a great demand to manufacture piles using materials that can be more durable compared to traditional materials especially in harsh environments. From 1987, several common types of composite piles have been developed including reinforced plastic piles, concrete filled Fibre-Reinforced Polymer (FRP) piles, fiberglass pultruded piles, fiberglass reinforced plastic piles, FRP hollow piles and FRP sheet piles (Guades et al., 2012). Although, FRP materials may cause some complications associated with pile driving and high damping, however, these materials can be a great option in aggressive corrosive environments. Concrete filled FRP tubes were used as a substitute to precast piles for Route 40 highway bridge over Nottaway River in Virginia (Fam et al. 2003). Several large FRP pipes were also installed in Eastern Canada and the United States to substitute old timber-stave pipes to transport water into turbines of hydroelectric plants (Bryden et al. 2014).

Most past studies on FRP piles were focused on the load transfer and flexural response of FRP piles under static loading. For example, Iskander et al. (2001) developed a theoretical parametric study on the effect of various pile properties and soil deposit conditions on driveability of FRP piles. Results of these analyses revealed that composite piles may well be driven to reasonable capacities for load-bearing piles. Helmi et al. (2006) studied the influence of driving forces and high-cycle fatigue on flexural performance of concrete-filled glass/carbon-FRP piles (GFRP and CFFT) and reported that driving forces may have minor influence on the flexural strength of CFFT piles. Concrete filled CFRP tubes with fibre orientation along the length of the pile were also reported to demonstrate higher load carrying capacity whereas the unconfined concrete piles reached lower capacity (Murugan et al. 2017). However, behaviour of FRP piles under seismic loading has not been well understood. Hence, this paper investigates the seismic response of hollow Glass FRP group piles compared to traditional group piles using shaking table tests. A series of shaking table tests with several shaking excitation inputs from the 1995 Kobe Earthquake and 2010 Central Canada Earthquake were carried out to evaluate seismic behaviour and the soil-pile

interaction of embedded end-bearing GFRP and aluminium group piles in dry sand.

## 2 EXPERIMENTAL PROGRAM

### 2.1 Model Testing Container

The shaking table tests were performed on a 1g shake table located at Civil and Environmental Engineering laboratory of Carleton University. This shaker system is a high-performance servo-hydraulic shaker used to apply 1-D horizontal base input displacement to models and model containers in response to an applied input voltage signal. The table can accommodate a maximum load of 10 tons and a maximum peak to peak displacement of 500 mm at the nominal operating frequency range of 0-50 Hz. A laminar shear container with dimensions of 1.0 meter by 1.0 meter with a height of 1.0 meter was used to contain the soil model. A thin latex membrane with thickness of 0.5 mm was fabricated and stretched inside the container to seal the laminar shear box (Figure 1).

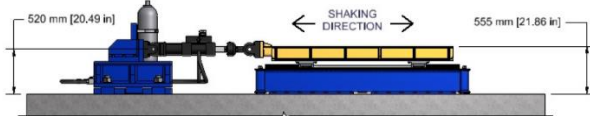
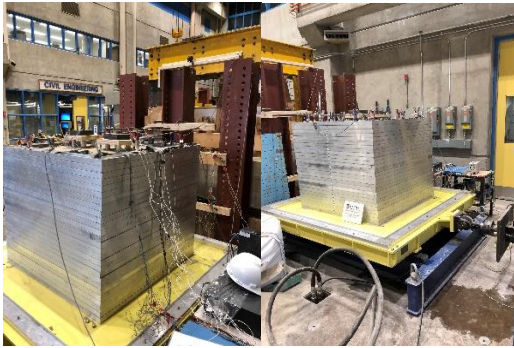


Figure 1: Shake Table in Civil Engineering Lab, Carleton University

### 2.2 Material Characterization

A poorly graded sand (SP) (Figure 2) was used to simulate the soil model and explore the seismic performance of FRP piles and conventional piles in cohesionless soils. The maximum dry density of the soil was measured at  $1.67 \text{ Mg/m}^3$  with the optimum water content of 10.8% as per ASTM D698 for standard Proctor test.

The ultimate tensile strength of the glass fiber-reinforced polymer was measured at 575 MPa, while its modulus of elasticity was about 17,000 MPa. The ultimate tensile strength of the aluminum tube used here to simulate the traditional pile materials was about 110 MPa and its yielding tensile strength and elastic modulus were estimated as of 95 MPa and 69,000 MPa respectively.

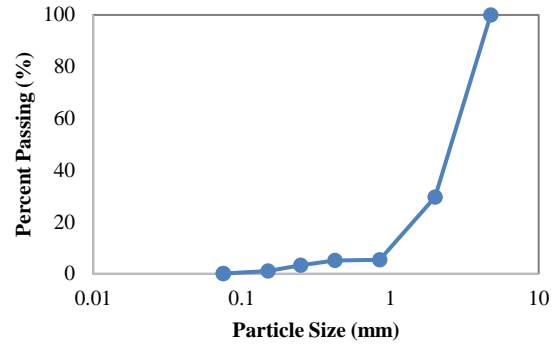


Figure 3: Particle size distribution of the test soil

### 2.3 Preparation of Model Piles and Pile Groups

A series of model GFRP piles were manufactured with commercially available glass fibre-reinforced fabrics used for reinforcement and retrofit of structural members. The model glass FRP piles were manufactured by fitting the glass fiber sheets around a steel tube. The fibre sheets were saturated in epoxy prior to fitting around the steel tube. After 48 hours of curing time, the piles were extracted from the steel tube and cut to the required length. Figure 3 illustrates the final configuration of all model piles along with the fabricated group piles. The group piles consisted of four (2 by 2) hollow GFRP or Aluminium piles with ... diameter. Piles within the group are distanced at approximately 200 mm from each other. Pile caps were loaded by lead weights of approximately 9 kg which was tightened by passing a threaded steel rod to keep the structural load fixed.

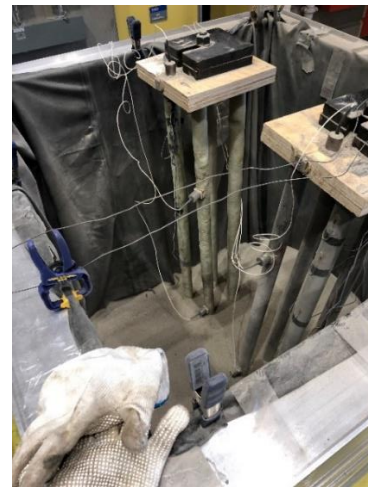


Figure 3: 2 by 2 Group Piles of Glass Fibre-Reinforced Polymer Piles and Aluminium Pile

### 2.4 Model Soil Preparation

Model soils in this experiment were prepared following sand raining through a series of sieves placed over the laminar shear box. The soil was initially oven dried and then

was rained (similar to pluviation method) slowly and uniformly inside the shaking shear box as shown in Figure 4. A series of small containers were placed at various locations and depths within the soil box to monitor the soil density and ensure uniform density throughout the soil model.

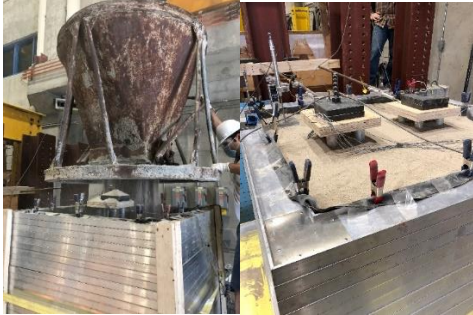


Figure 4: Sand preparation steps

## 2.5 Instrumentation and Testing Procedure

Several instruments and sensors including accelerometers, LVDTs and strain gauges were positioned within the soil and mounted on piles and pile caps to collect the test data. Two accelerometers were positioned at depths of 200 mm and 800 mm within the soil layers to record the free field motions in the soil. Similarly, 2 accelerometers were installed on a pile per each group at the same depths as the free field accelerometers to measure the pile-soil interaction effects. Also, one accelerometer was mounted on the pile cap of each group pile and head masses to detect possible translation and rocking motions. String potentiometers were also fastened to the laminar box at depths of 200 mm and 800 mm to record the displacement along the laminar box, and additionally 2 LVDTs were mounted on pile caps to record any potential flexibility induced by the piles during shaking. Furthermore, another LVDT was positioned vertically on top of the soil to record the soil settlement during each shake test. Lastly, a total of eight bending strain gauges were mounted on both sides of individual piles in each group to measure the strain and consequently the change in bending moment of the piles during the shaking tests (Figure 5).

The input ground motions recorded during the 1995 Kobe Earthquake and the 2010 Central Canada Earthquake were used in this research. Each test model was subjected to 3-6 near-field shaking events at intensity of 50%, 100%, and 200%.

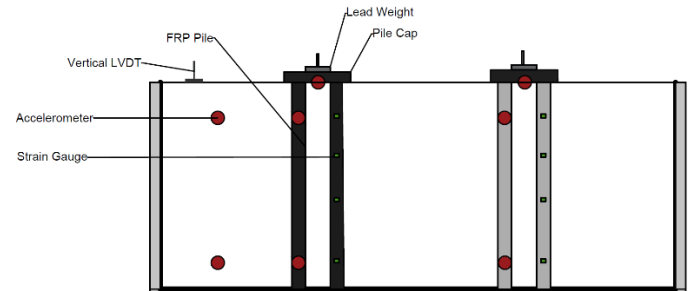


Figure 5: Instrumentation locations inside the laminar soil container of the shaking table

## 3 TEST RESULTS AND DISCUSSION

### 3.1 Acceleration Time Histories

Peak accelerations in terms of 'g' at the accelerometer locations for both pile groups are presented in Table 1. A2 and A3 are accelerometers attached to a pile per group near the base; A5 and A6 are mounted on the pile at a depth close to the surface; A1 is located in free field close to the base; A7 and A8 are mounted on the structure. From the time histories of acceleration, the soil conditions had an essential effect on the site response, as expected. The peak accelerations are typically assumed to illustrate an increasing trend from the base to the surface; however, this statement is not true for GFRP group piles.

The distribution of acceleration varies along the shaft of both GFRP and Aluminum group piles. The GFRP group pile experienced larger acceleration close to its base and followed by a reduction in peak acceleration near the surface and eventually lower acceleration was felt at the pile cap of GFRP pile. However, this trend was different for the Aluminum group piles. The Aluminium group pile cap experienced higher acceleration compared to the GFRP group pile cap. This also means that superstructure rested on Aluminum group piles would have experienced significantly greater acceleration in traditional piles. This can be referred to the higher stiffness of the traditional pile group and hence more significant kinematic soil-pile-structure interaction. The higher peak accelerations in the Aluminum pile cap may also result in excitation of the base shear, moment and torsion, which consequently can appear as displacement and rotation of the foundation relative to the free field.

Furthermore, the recorded peak accelerations within the soil (free field) for all applied excitations were significantly less than those measured on piles at the same depth. This difference in peak ground motions underscores the importance of considering soil-pile interaction impacts on foundation input motions in seismic prone areas. The difference between the free field and pile motion is significantly lower for the GFRP pile group compared to the traditional Aluminium pile group. This behaviour is also attributed to the lower rigidity and higher flexibility of the GFRP piles, which leads to lower motions and closer acceleration level to those measured in the soil (free field motion).

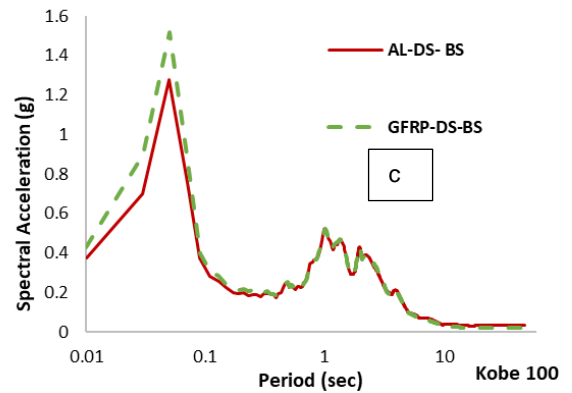
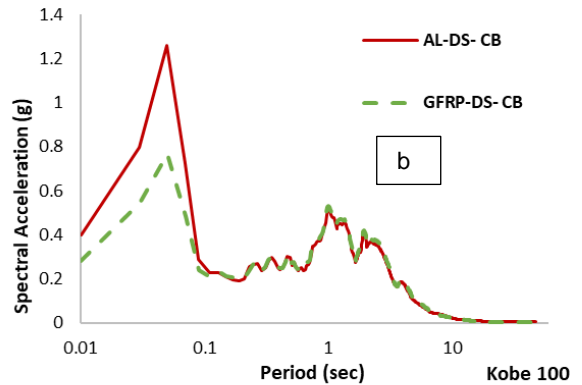
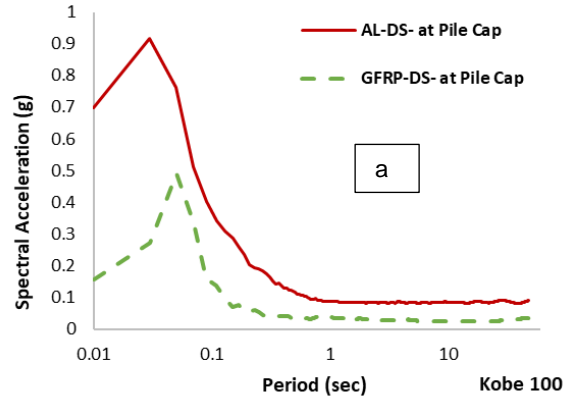
Table 1: Summarized peak accelerations of shaking table tests in dry sand

Model Pile	Input motion (g)	A1	A2/ A3	A5/ A6	A7/ A8
GFRP (DS)	O50	0.007	0.011	0.009	0.012
	O100	0.086	0.624	0.665	0.388
	O200	0.151	0.952	0.862	0.358
	K50	0.060	0.242	0.245	0.118
	K100	0.100	0.412	0.432	0.388
	K200	0.157	0.932	0.889	0.344
AL (DS)	O50	0.007	0.007	0.005	0.011
	O100	0.086	0.660	0.685	1.276
	O200	0.151	0.922	0.960	1.954
	K50	0.060	0.164	0.237	0.655
	K100	0.100	0.292	0.397	1.377
	K200	0.157	0.909	0.938	1.945

A1 free field motion inside soil near the base  
 A2 (GFRP) and A3 (Aluminum, AL) close to base (CB)  
 A5 (GFRP) and A6 (Aluminum, AL) beneath the surface (BS)  
 A7 (GFRP) and A8 (Aluminum, AL) mounted on the pile cap/structure.

### 3.2 Spectral Acceleration

Spectral analysis is used to describe the frequency content of the input motions measured on the piles and within the soil. Response spectra of the motions can also be used to assess the ground motion amplification and seismic hazard associated with different earthquake motions. The response spectra of the pile models for the Kobe events of K100, and K200 are illustrated in Figure 6 (a, b, and c) with a constant damping ratio of 5%. Similar to acceleration time histories, the seismic motions measured on the pile cap of Aluminium piles have experienced higher amplifications compared to the GFRP pile cap. Most these amplifications were recorded at a period of 0.05-0.1 seconds, corresponding to the frequency range of 10-20 Hz. The frequency content of the amplified motions seems to be consistent for both the model pile groups. Therefore, the soil-pile interaction has not deviated the frequency range of seismic motions recorded for both the pile systems and only amplified the input motion.



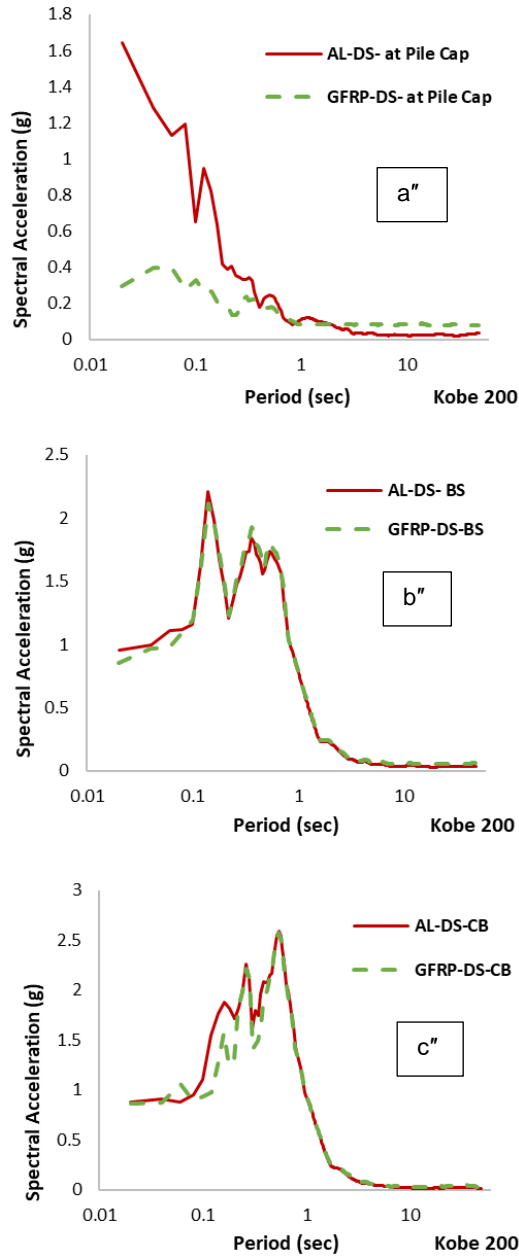


Figure 6: Response Spectra for all piles (GFRP, and aluminium) under exciations of K100, and K200

### 3.3 Kinematic Soil-Structure Interaction

The kinematic interaction can occur due to embedment of rigid foundation elements within the soil. This will potentially deviate the foundation motions from free field motions. As a result, this may cause wave inclination, or foundation rocking due to base-slab averaging and embedment effects (Stewart et al., 1999). This interaction can be defined as frequency dependant transfer function involving both the free field motion and the base-slab motion while the base and structure are assumed massless. The relationship between the shaking periods of the model pile

and the supporting soil influences the seismic response of the structures. Figure 7 shows the ratio of response spectra (RRS) curves, obtained by normalizing the acceleration response of the model piles close to the base (CB) over the free field acceleration situated at the same depth under K200 shaking. The result demonstrates very similar trend and peak to peak behavior for the GFRP group piles and Aluminium group piles. However, the RRS values for the GFRP piles are less than those for the Aluminium piles for the period range of 0.1-0.5 seconds, showing higher soil-structure interactions for the traditional piles.

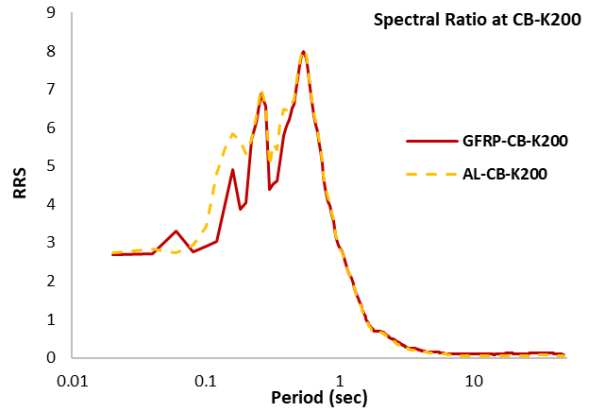


Figure 7: Ratio of response spectra for all models during K200 shaking event

### 3.4 Bending Moment

A series of bending strain gauges were used to measure the strain and in turn bending moments of the piles during the tests. As stated by the theory of elasticity and Hooke's law (Timoshenko, 1940), the generated moment in the pile section is a function of the recorded strain in the strain gauges, referring to the following equation:

$$M = \frac{2EI}{D} \times \varepsilon \quad [1]$$

where,  $E$  is the modulus of elasticity,  $I$  is defined as the moment of inertia,  $D$  is the outer diameter of the pile, and  $\varepsilon$  is the recorded strain in the strain gauges. Figure 8 illustrates the bending moment along the pile shaft for both the pile groups (GFRP, and aluminium) at K200 shaking event. The distribution of the moment amplitude along the pile shows that the bending moments are larger at the upper section of the GFRP piles while smaller bending moments were generated at the top section of Aluminium piles. Overall, Aluminum piles have experienced lower bending along their shaft which is due to higher rigidity of these piles. On the other hand, GFRP piles have shown higher bending moment, indicating higher flexibility of GFRP materials.

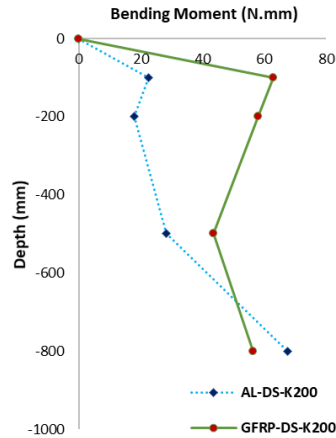


Figure 8: Recorded bending moment distribution along the piles at K200

#### 4.0 SUMMARY AND CONCLUSIONS

From the results of this study, the following conclusions may be drawn in this shaking table test program:

- The peak accelerations measured for the GFRP pile group was significantly less than those recorded for the traditional Aluminium piles. This behaviour is attributed to lower rigidity of the GFRP piles compared to traditional piles.
- The frequency content of the amplified motions appears to be consistent for both the model pile groups. Therefore, the soil-pile interaction has not deviated the frequency range of seismic motions recorded for both the pile systems and only amplified the input motion.

#### Acknowledgements

This study was financially supported by Natural Sciences and Engineering Research Council of Canada (NSERC).

#### REFERENCES

ASTM D698-12e1. (2012) Standard Test Methods for Laboratory Compaction Characteristics of Soil Using Standard Effort (12 400 ft-lbf/ft<sup>3</sup> (600 kN-m/m<sup>3</sup>)), ASTM International, West Conshohocken, PA.

Fam, Amir Z. and Miguel A. Pando. (2003). "Precast piles for Route 40 bridge in Virginia using concrete filled FRP tubes." *PCI Journal*, vol. 48, (3), pp. 32-45.

Fam A., Boles R., and Robert M. (2016). "Durability in a Salt Solution of Pultruded Composite Materials Used in Structural Sections for Bridge Deck Applications," *Journal of Bridge Engineering*, vol. 21, (1), pp. 4015032.

Guades, E., Aravinthan, T., Islam, M. and Manalo, A., 2012. A review on the driving performance of FRP composite piles. *Composite Structures*, 94 pp. 932-1942.

Helmi K., Fam A., Mufti A., and Hall J. M., 2006. Effects of driving forces and bending fatigue on structural performance of a novel concrete-filled fibre-reinforced-polymer tube flexural pile. *Can. J. Civ. Eng.* 33: 683–691.

Iskander, M. G., Hanna, S. and Stachula, A., 2001. Driveability of FRP Composite Piling. *Journal of Geotechnical and Geoenvironmental Engineering*, 127, pp. 169-176.

Mogami, T., and Kubo, K., 1953. "The Behaviour of Soil During Vibration" *Proceedings of the Third International Conference on Soil Mechanics and Foundation Engineering*, Vol. 1, pp. 152-153.

Murugan, M., Muthukkumaran, K., & Natarajan, C. (2017). FRP-strengthened RC piles. I: Piles under static lateral loads. *Journal of Performance of Constructed Facilities*, 31(3), 4017003. Doi:10.1061/(ASCE)CF.1943-5509.0000990.

Stewart, J.P., Fenves, J.L. and Seed, R.B. (1999). Seismic soil-structure interaction in buildings. I: Analytical methods. *Journal of Geotechnical and Geo-environmental Engineering*, Vol. 125, No. 1, pp: 26-37.

Timoshenko, S. (1940). *Strength of materials (2<sup>nd</sup> ed)*. D. Van Nostrand Company, Inc, New York.